IEEE Access
Multidisciplinary ⋮ Rapid Review ⋮ Open Access Journal

Received 18 October 2023, accepted 8 November 2023, date of publication 13 November 2023, date of current version 16 November 2023.

Digital Object Identifier 10.1109/ACCESS.2023.3332116

RESEARCH ARTICLE

Machine Learning Based Recognition of Elements in Lower-Limb Movement Sequence for Proactive Control of Exoskeletons to Assist Lifting

JONG-HA WOO[1], K. KRISHNA SAHITHI[1], SEONG-TAEK KIM[1], GEUN-RYEONG CHOI[1], BEOM-SU KIM[1], JONG-GYU SHIN[2], AND SANG-HO KIM[1]

[1]Department of Industrial Engineering, Kumoh National Institute of Technology, Gumi 39177, South Korea
[2]Research Institute of Industrial Engineering and Management, Kumoh National Institute of Technology, Gumi 39177, South Korea

Corresponding author: Sang-Ho Kim (kimsh@kumoh.ac.kr)

This work has supported by a National Research Foundation of Korea (NRF) grant funded by the Korea government [Ministry of Science and ICT (MSIT)] (No. 2021R1A2C2095410).

This work involved human subjects in its research. Approval of all ethical and experimental procedures and protocols was granted by the Institutional Review Board (IRB) of Kumoh National Institute of Technology under IRB No. 202110-FR-016-02.

ABSTRACT Exoskeleton robots that provide physical assistance to workers at industrial sites have recently been advanced by utilizing various bio-signal measurement sensors and artificial intelligence. However, their commercialization speed is slow compared to the pace of technological development. One of the reasons for this is the motion mismatch that occurs between the control of the exoskeleton and the worker's response. To solve this issue, the worker's intended motion could be predicted, and proactive control of the exoskeleton robot could be implemented. An experiment was conducted with 35 subjects, with the data of 30 subjects used for unsupervised learning and the data of the remaining 5 subjects used for supervised learning. To predict the intended motion of the subjects, the data from IMU sensors were used to segment the motion elements through a k-means clustering algorithm, employing a motion segmentation technique. The lower extremity motion was understood as a sequence composed of motion elements. The potential for predicting motion intention and sequence was demonstrated by comparing the results from unsupervised learning with those of an MLP model that predicted motion sequences from new, unused data. Additionally, it was confirmed that proactive control of the exoskeleton robot using the motion segmentation technique was possible when the duration of the element motion constituting the lower extremity motion sequence exceeded 200ms. Therefore, this study conducted preliminary research to develop a system for predicting a worker's intended motion and motion sequence for proactive control of an exoskeleton robot.

INDEX TERMS Machine learning, exoskeleton, proactive control, human–robot interaction, motion segmentation.

I. INTRODUCTION

Exoskeleton devices enhance the physical abilities of non-disabled wearers [1]. Moreover, they combine machine power and human intelligence to augment machine intelligence and provide power to the operator by working in parallel with the human body, either passively or actively [2].

The associate editor coordinating the review of this manuscript and approving it for publication was Tao Liu.

They are also referred as wearable robots with close physical and cognitive interaction with the operator [3]. Additionally, industrial exoskeletons aim to reduce fatigue and injuries while increasing work performance in manufacturing and production environments. These exoskeletons are particularly suitable for assisting workers in performing repetitive tasks in challenging postures, such as bending, squatting, or reaching for overhead objects [4]. Despite the rapid development of exoskeletons that provide physical assistance to workers, their commercialization speed is slow. Despite the anticipated industry benefits of exoskeletons, factors such as high purchase costs, inconvenience arising from improper fitting of the exoskeleton device to the worker's body [4], and discomfort caused by inadequate control, which results in a mismatch between the assistant force and the worker's intentions, hinder their widespread adoption. Furthermore, inconveniences arise when the control of the exoskeleton lags behind the worker's intended motion.

The primary obstacle to the fast commercialization of the exoskeleton may be that users feel uncomfortable wearing the device due to the delay between the start of control and their intended movements. This problem occurs due to the time difference between the human acting immediately following the intention of motion and the robot following later due to control delay, which increases the risk of injury [5]. Additionally, there is always a time delay due to motion detection time, data operation processing time, and control response time to control the exoskeleton, and this time delay makes the human-in-the-loop control unstable [6]. Therefore, to solve the motion mismatch problem, predicting the intention of motion and reducing the control delay time through proactive control could be a solution.

As the exoskeleton robot is controlled based on the measurement of human movement and force, controlling the exoskeleton by predicting movement based on bio-signals can reduce control delay [6]. Therefore, to predict the motion intention of a human, it is necessary to collect bio-signals using sensors. Sensors for bio-signal measurement include the electroencephalogram (EEG) [7], electrooculography (EOG) [8], electromyogram (EMG) [9], inertial measurement unit (IMU), and insole sensors. Among them, the EMG, IMU, and insole sensors are mainly used to perform proactive control of the exoskeleton. Therefore, it is possible to solve the motion mismatch problem by predicting the operator's intended motion and using sensor data to implement proactive control of the exoskeleton robot.

To implement proactive control of the exoskeleton robot using sensor data, first, it is necessary to identify motion sequence elements through a motion segmentation technique. Dividing one entire movement into several small movements allows researchers to understand them as a series of sequences. In particular, applying motion segmentation techniques and using data expressed in sequences to teach robots human movement techniques can effectively find motion primitives [10]. By understanding motion as a sequence using the divided elements, human motion can be predicted based on the order in which the elements change. Second, it is necessary to predict movement intention using sequences composed of segmented components of lower extremity movements. This is to compensate for the control delay time of the exoskeleton robot and ensure synchronicity between human motion and exoskeleton control. In order to predict movement intention, it is necessary to utilize characteristics of muscle activities detected using an EMG sensor. In particular, movement intention involved in performing lower limb movements can be identified using the relationship between agonist and antagonist muscles. In addition, it is believed that through IMU and EMG multimodal sensors, the mechanism of actual human movement can be simulated using the angle/angular velocity/angular acceleration of lower extremity joints and contraction data of lower extremity muscles. Through this, it will be possible to develop a proactive control algorithm for a multimodal sensor-based exoskeleton robot. Third, it is necessary to check and verify whether the exoskeleton robot is properly controlled when the proactive control algorithm is applied to the exoskeleton robot. It is also stated by Akbari et al. in [11] that deep learning algorithms do not statistically guarantee reliable performance for various scenarios. It was also noted that safety issues are highlighted in that there are limitations in processing data that fall outside the learning distribution. Accordingly, it will be necessary to verify safety aspects by applying the algorithm to an exoskeleton robot. In particular, because the exoskeleton is a wearable type, if the algorithm incorrectly predicts the operator's movement intention and a malfunction occurs, it can immediately lead to injury. For this reason, before experiments with humans, the algorithm's performance must be verified through methods such as humanoid robots and simulations and then applied to the exoskeleton robot to ensure safety. Lastly, we aim to minimize the number of attached sensors by simplifying the use of sensors by just using vision-based sensors. This is because once exoskeleton robots are commercialized and used in industrial settings, it is difficult to attach many sensors to the body individually.

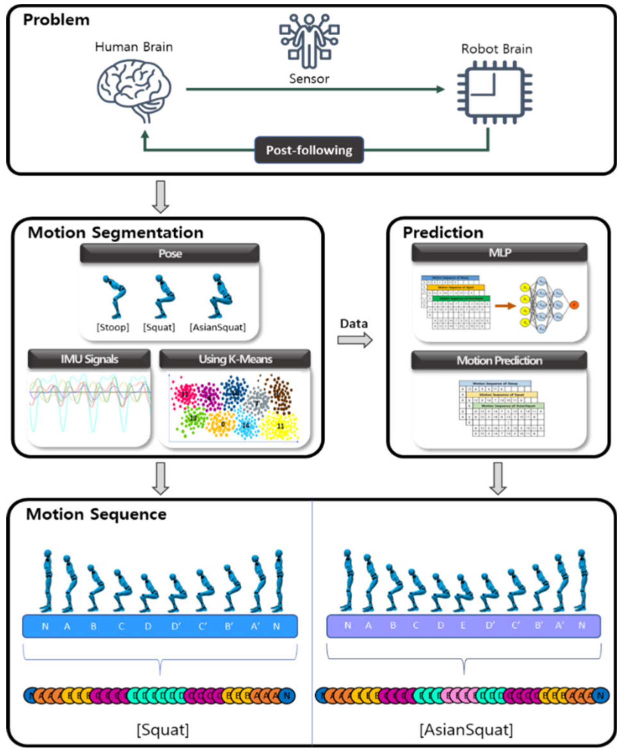

FIGURE 1. Overall research framework.

Accordingly, we went through a process of verifying whether the IMU sensor would show the same performance as the existing model even if it was replaced with a vision sensor instead of the EMG sensor that must be attached. As a result, we wanted to develop a system for predicting operator movement intention and sequence for proactive control of exoskeleton robots.

This study presents a preliminary exploration for the development of the final step mentioned above. Hence, in this study, a motion segmentation technique was applied to solve the motion mismatch problem by dividing the lower extremity motion into elements and understanding the segmented lower extremity motion elements as a sequence. Through this, we intend to verify the research concept for predicting sequences of lower extremity movements and adopt it as a research method. Based on the three representative movements of the lower extremity, Stoop/Squat/Asian Squat, biometric data were collected using a single IMU sensor, and the lower extremity movements were divided through unsupervised learning. Moreover, supervised learning was performed to test the feasibility of developing a motion intention prediction model. The predictability of motion sequences was confirmed by comparing the results with those of unsupervised learning.

II. RELATED WORK

To solve the motion mismatch problem, we propose implementing proactive control through motion intention prediction. To this end, if the entire motion can be understood as a sequence of elements of the lower extremity motion, motion intention prediction can be effectively performed. Most studies have identified or classified human movements by performing motion segmentation using video data sets. To improve the performance of systems that can detect, recognize, and synthesize human motion for virtual reality, smart surveillance systems for advanced user interfaces, motion analysis for segmentation was performed by applying deep learning/machine learning algorithms to open video datasets such as the CMU, HDM05, Cornell, Keck, Weizmann, MAD, and KTH datasets [12], [13], [14], [15], [16]. Furthermore, data measured by the motion capture system for continuous motions such as walking and ballet motions were divided into 15 motion primitives for ballet motions and 10 motion primitives for walking motions using motion segmentation techniques [17]. The studies reviewed above proposed efficient motion segmentation solutions based on artificial intelligence algorithms; however, their solutions used data captured from video images. The exoskeleton must be designed to collect and control data in real-time, and it is not very easy to conduct proactive control by using video datasets. Hence, it was determined that the bio-signal data of the wearer should be used directly. In particular, in the learning approach to imitate human motion, it is common to record and process data using various sensors (e.g., IMU, EMG, insole, motion capture, etc.) [18]. In addition, bio-signal data can accurately measure human body kinematics, identify aspects that cannot be found in image data, and enhance the understanding of motion [19]. Therefore, it is necessary to confirm studies on motion segmentation using bio-signal data.

Beil et al. [20] achieved an average classification accuracy of 92.8% through an HMM motion classification system using data acquired from three IMU sensors and seven 3D-force sensors. Zhang et al. [21] proposed a Bag of Features framework using IMU sensor data extracted from nine different activities and segmented motions into motion primitives using a k-means clustering algorithm. Santikan et al. [22] collected data with an IMU sensor and performed motion segmentation using the k-means clustering algorithm to classify the walking patterns of healthy and disabled people according to their gait cycles. The above studies understood human movement by dividing and classifying the entire movement. In particular, Naghdy and Fazel [10] applied IMU sensor data to a Fuzzy Clustering algorithm to develop a general approach to teach human movements to humanoid robots. Furthermore, hand movements were segmented into six motion primitives and expressed them as sequences. This study used the motion segmentation technique to break down an entire movement as a sequence. The technique used in this study is based on the research method used by Naghdy and Fazel [10]. However, our study gathered a considerable amount of experimental data, and we have also increased the number of features used. There is also a need to check the possibility of developing a motion intention prediction model for proactive control of an exoskeleton robot using sensor data.

We reviewed studies that used more than one type of sensor to acquire bio-signal data and classified and predicted human motion through the data they acquired. Trotora et al. [23] predicted motion through the GMM model using IMU and EMG data, and Ding et al. [6] predicted gait for exoskeleton control through motion intention prediction using the IMU and insole sensors. Previous studies [6], [23] have produced effective results using multimodal sensors. However, Stolyarov et al. [24] performed gait prediction using an IMU sensor and an sEMG sensor but the accuracy of the IMU sensor was higher, and that of the sEMG sensor was affected by factors such as sweat, skin temperature, and thickness of subcutaneous fat. Based on the variability of the signal, we emphasized the need to use IMU sensor data and, at the same time improve the performance using only the IMU sensors to predict motion intention. Fang et al. [25] stated that the movements of a human and the exoskeleton need to be sufficiently synchronized and conducted research based on IMU sensor data to optimize human-exoskeleton interaction and perform gait prediction. Therefore, motion classification and prediction can be effectively performed using a single IMU sensor. Hence, in this study, first, the research method was established using just the IMU sensors, and the possibility of developing a proactive control model using the motion segmentation technique remains to be confirmed.

The studies reviewed above [10], [20], [21], [22] used various algorithms to segment motions; however, most used k-means clustering-based algorithms. Data clustering is a method of creating groups of objects or clusters so that similar objects are grouped and different objects are separated into distinct clusters. Many clustering algorithms, but the k-means clustering algorithm is the most important and widely used [26]. In particular, pattern classification is performed in human motion studies using temporal motion data and the k-means clustering algorithm [26]. This indicates that the algorithm is mainly used for human motion research and offers the added benefits of ease, speed, and scalability for processing large datasets. Therefore, motion segmentation was performed in this study using the k-means clustering algorithm.

The lower extremity motion elements obtained using the above algorithm are expressed and understood as a sequence to prepare the basis for proactive control. This means it is necessary to secure high accuracy when predicting new data by training the supervised learning model based on the result derived through unsupervised learning. Therefore, we use the multi-layer perceptron (MLP) model, which is one of the commonly used neural network architectures owing to its low complexity and ability to produce satisfactory results for nonlinear relationships [27]. Liu et al. [28] proposed an MLP-based model capable of detecting gait phases in real-time for application to exoskeleton robots, accurately predicting gait phase labels. Although the MLP algorithm is a commonly used algorithm, it is only used for real-time control of the exoskeleton and has powerful performance. Therefore, in this study, the possibility of proactive control is confirmed using MLP, a supervised learning model.

III. RESEARCH METHODS

A typical task in industrial settings that requires a high level of lower extremity muscle strength is heavy lifting work. The postures involved in manual lifting work are Stoop/Squat/Asian Squat, where workers perform these three movements sequentially, and each movement applies different loads to the joints of the lower extremity [19]. Classifying these three motions is particularly challenging due to individual differences in human motion and posture [19]. Therefore, in this study, we aimed to include a broader range of lower extremity motions compared to previous studies by adding the Asian Squat, which involves more lower extremity joints, along with Stoop/Squat. The overall experiment framework consisted of three steps: (1) data collection and preprocessing, (2) clustering of lower extremity motion elements, and (3) model verification using machine learning. We collected data for the lower extremity using only IMU sensors. We segmented the motion by applying the unsupervised k-means clustering algorithm to identify the elements of lower extremity motion. The segmented motion was then represented and understood as a sequence, and the labeled data was used to train an MLP model. The results were compared with the results of unsupervised learning, and the feasibility of proactive control was determined through motion prediction using the MLP model.

TABLE 1. Degrees of freedom (DoF) of each joint from IMU sensor.

No	Joint	DoF	Movement
1	Hips	3	Flexion – Extension
			Abduction – Adduction
			Rotation
2	Knees	2	Flexion – Extension
			Rotation
3	Ankles	2	Flexion – Extension
			Eversion – Inversion

A. DATA COLLECTION

A total of 35 healthy males in their 20s and 30s who regularly exercise were recruited to participate in this study. The subjects had an average height of 176.6 (±4.9)cm and an average weight of 78.9 (±11.1)kg. The experiment involved performing 60 or 50 Stoop/Squat/Asian Squat movements per subject, with four subjects participating in the pilot test, resulting in a total of 180 or 150 movements. To minimize physical burden and fatigue, the experiment was divided into 12 sets, each consisting of 15 repetitions per movement. After completing the first set, a 5-minute break was provided. Before commencing the experiment, the subjects received training on the experimental motions to minimize individual differences. Throughout the experiment, an operator monitored and guided the posture of the subjects. The entire experiment was recorded using AVARTAR provided by the CAPTIV-L7000 software for subsequent data analysis. Prior to the start of the experiment, consent was obtained from all subjects. The purpose of the experiment and the collection/use of biometric data were explained to the participants. This study was conducted with the approval of the Institutional Review Board (IRB) of Kumoh National Institute of Technology (IRB approval number: 202110-FR-016-02, approval date: September 6, 2022).

B. SENSOR NETWORK

IMU sensors are widely used for measuring human motion [5]. In this study, the TEA's CAPTIV T-Sens Motion IMU Sensor was chosen considering wearability and usability. It allows wireless communication, and the sampling rate was set to 64 Hz. Since each joint of the body has a different range of motion or degree of freedom [29], Table 1 provides details about the measurable degrees of freedom for the IMU sensor used in the experiment.

The hip, knee, and ankle are the joints in the lower extremities of the human body, each with different capabilities and degrees of freedom. Consequently, the exoskeleton actuators for the lower extremities can only be driven by the hip, knee, and ankle joints [29], and the attachment locations for the IMU sensors need to be determined based on the recommendations in TEA's user guide. For this experiment, a total of

TABLE 2. Degrees of freedom (DoF) of each joint from IMU sensor.

Movement	Feature		
	Angle	Speed (Angular Velocity)	Acceleration
Flexion - Extension	(Left / Right) Hip (Left / Right) Knee	(Left / Right) Hip (Left / Right) Knee	(Left / Right) Hip (Left / Right) Knee
Abduction - Adduction	(Left / Right) Hip (Left / Right) Ankle	(Left / Right) Hip (Left / Right) Ankle	(Left / Right) Hip (Left / Right) Ankle
Rotation	(Left / Right) Hip (Left / Right) Knee	(Left / Right) Hip (Left / Right) Knee	(Left / Right) Hip (Left / Right) Knee
Eversion - Inversion	(Left / Right) Ankle	(Left / Right) Ankle	(Left / Right) Ankle

TABLE 3. Eighteen selected features.

No	Feature	Movement	No	Feature	Movement
1		Left Hip (Flexion - Extension)	10		Right Hip (Flexion - Extension)
2	Angle	Left Knee (Flexion - Extension)	11	Angle	Right Knee (Flexion - Extension)
3		Left Ankle (Flexion - Extension)	12		Right Ankle (Flexion - Extension)
4		Left Hip (Flexion - Extension)	13		Right Hip (Flexion - Extension)
5	Speed	Left Knee (Flexion - Extension)	14	Speed	Right Knee (Flexion - Extension)
6		Left Ankle (Flexion - Extension)	15		Right Ankle (Flexion - Extension)
7		Left Hip (Flexion - Extension)	16		Right Hip (Flexion - Extension)
8	Acceleration	Left Knee (Flexion - Extension)	17	Acceleration	Right Knee (Flexion - Extension)
9		Left Ankle (Flexion - Extension)	18		Right Ankle (Flexion - Extension)

seven sensors were attached to the waist, the center of the thigh (right/left), the center of the calf (right/left), and the top of the foot (right/left). An illustration of the sensor attachment on an actual subject can be seen in Figure 2 below.

Prior to the experiment, the baseline readings of the seven IMU sensors were taken to minimize errors caused by the sensors themselves. After attaching the sensors to the subjects, synchronization between the software and the subjects was performed twice, once in the standing posture and once in the squat posture.

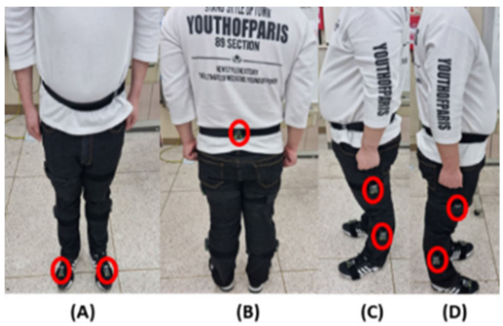

FIGURE 2. Placement of IMU sensors: (A) frontal view; (B) rear view; (C) left side view; and (D) right side view.

C. DATA PROCESSING

A total of 42 features could be extracted from the data obtained from the IMU sensor, as shown in Table 2. These features were calculated by determining the angle, speed (angular velocity), and acceleration values for each degree of freedom described in Table 1. The feature data was exported from the software and saved as a.csv file. Python was utilized for data analysis, Pandas for data handling, the scikit-learn module for unsupervised learning, and TensorFlow for supervised learning.

To prevent bias in the clustering results caused by features with larger numerical sizes [10], various normalization methods were applied to the raw data. Among all the methods, min-max normalization, which empirically exhibited the best performance, was selected. This method converts the data to a value between 0 and 1. The pre-processed data, with added labels to distinguish motions, was used for analysis. Additionally, the data from 30 subjects was integrated into a single file.

D. DATA PROCESSING

Motions can be manually segmented by determining the range of each feature using the data acquired from the IMU sensor. However, in this case, the algorithm performed motion segmentation directly and identified the characteristics of the segmented motions. Therefore, 18 features were empirically selected by altering the feature combinations to identify the features that can yield good results, as shown in Table 3.

Next, the data of 30 out of the 35 individuals were used for preprocessing. Subsequently, unsupervised learning was

TABLE 4. MLP model structure.

Layer	Neurons
Input	18
Hidden1 (ReLU)	1024
Hidden2 (ReLU)	512
Hidden3 (ReLU)	256
Hidden4 (ReLU)	128
Hidden5 (ReLU)	64
Output (Softmax)	8/10/12/16/18

TABLE 5. MLP model structure.

Parameters	Values
Batch Size	64
Loss Function	Mean Squared Error
Optimizer	Adam
Learning Rate	0.001
Epochs	10

conducted, and the cluster numbers were set to 8, 10, 12, 16, and 18 in order to find the optimal number of clusters with good clustering results. Finally, the results for each cluster setting were derived.

E. MOTION PREDICTION

Real-time control necessitates prediction using raw data without any data preprocessing. Consequently, the outcomes of unsupervised learning are employed to train a model, and new data is predicted using raw, unprocessed data to confirm accuracy. Initially, the results of unsupervised learning were utilized to train the MLP model, which consists of an input layer, five hidden layers, and an output layer, as illustrated in Table 4. The hyperparameter configuration for the model was set as follows: Loss Function: Mean Squared Error; Optimizer: Adam, as presented in Table 5. The effectiveness of the proactive control model was verified by predicting the clusters for the data of five individuals who were not involved in the unsupervised learning phase and subsequently comparing the results with those of unsupervised learning.

IV. RESULTS

A. DETERMINATION OF THE NUMBER OF CLUSTERS

By integrating motion data acquired through experiments, clustering labels (target) were obtained as a result of unsupervised learning. We defined the result as motion elements. The optimal number of clusters was determined by empirically comparing the results according to the number of clusters. The criterion for determining the optimal number of clusters was established by referring to the study of Hwang et al. [30]: (1) Cluster interpretation should not be complicated, and it was determined by visually examining the average and ratio data for all variables. (2) To determine the optimal number of clusters, the number of data points in each cluster was considered. This is because variability can increase if the amount of data in a cluster is less than 1000. (3) Each joint's range of motion (ROM) must be distinguishable among clusters. (4) While satisfying the above three conditions, it was determined that the number of motion elements constituting the motion sequence should be as large as possible, and the motion sequence classification rate should also be high.

As a result, it was confirmed that the classification performance was the best when clustering was performed with 16 clusters. The process of selecting the optimal number of clusters can be seen in Figure 3.

B. CLUSTERING OF MOTION USING UNSUPERVISED LEARNING

A total of 16 motion elements were identified through unsupervised learning. The motion sequence for each motion is illustrated in Figure 3. While Squat and AsianSquat exhibit a similar motion sequence, it can be observed that Stooping has a distinct sequence, with the exception of one step at the beginning and end. This difference is likely influenced by the posture adopted when lifting an object, despite Stooping primarily involving lower extremity motion.

Therefore, it was confirmed that 11 of the 16 clusters (6, 12, 0, 14, 7, 2, 8, 13, 3, 10, 11) corresponded to motion elements obtained using the motion segmentation technique. The remaining five clusters (4, 5, 1, 9, 15) were not considered as motion elements of the lower extremities because they were classified based on the IMU sensor data attached to the waist rather than the lower extremities. Additionally, it was determined that Stoop was not solely a lower extremity motion since elements 4, 5, 1, and 15 were included in the motions constituting Stoop.

Regarding the Squat and AsianSquat motions, the motion sequence was analyzed based on the motion elements' angle and speed (angular velocity) values. Figures 5 and 6 confirm the symmetry of the values in clusters 12-11, 0-10, 14-3, and 7-13. Figure 4 shows the classification of another motion element based on the change in angle value for each joint, influenced by posture changes and the positive or negative angular velocity of each joint. Specifically, clusters 12, 0, 14, and 7 correspond to going down while bending the knees from a standing posture, while clusters 13, 3, 10, and 11 represent returning to a standing posture. This classification makes it challenging to identify symmetrical motion elements from the perspective of exoskeleton control. Consequently, symmetrical motion elements are expressed within the same cluster, while the return to a standing posture is classified with a different symbol, as shown in Table 6.

C. TIME OF MOTION ELEMENT IN THE MOTION SEQUENCE

As a result of unsupervised learning, representative sequences expressing the Squat and AsianSquat movements were identified. In this study, motion was segmented to derive sequences and facilitate proactive control implementation.

TABLE 6. Before and after changing the symbols of motion elements.

Cluster	Before	6	12	11	0	10	14	3	7	13	2
	After	N	A	A'	B	B'	C	C'	D	D'	E
Right Knee Angle F/E	mean	4.92	17.21	15.04	45.30	39.57	74.73	68.30	98.61	97.18	124.96
	std	3.62	7.57	6.74	9.10	8.84	9.49	9.20	9.34	10.56	8.85
Left Knee Angle F/E	mean	4.66	18.35	16.17	46.63	40.80	75.68	69.65	99.65	98.54	126.67
	std	3.46	7.72	6.62	9.34	8.92	9.62	9.37	9.74	10.80	8.35

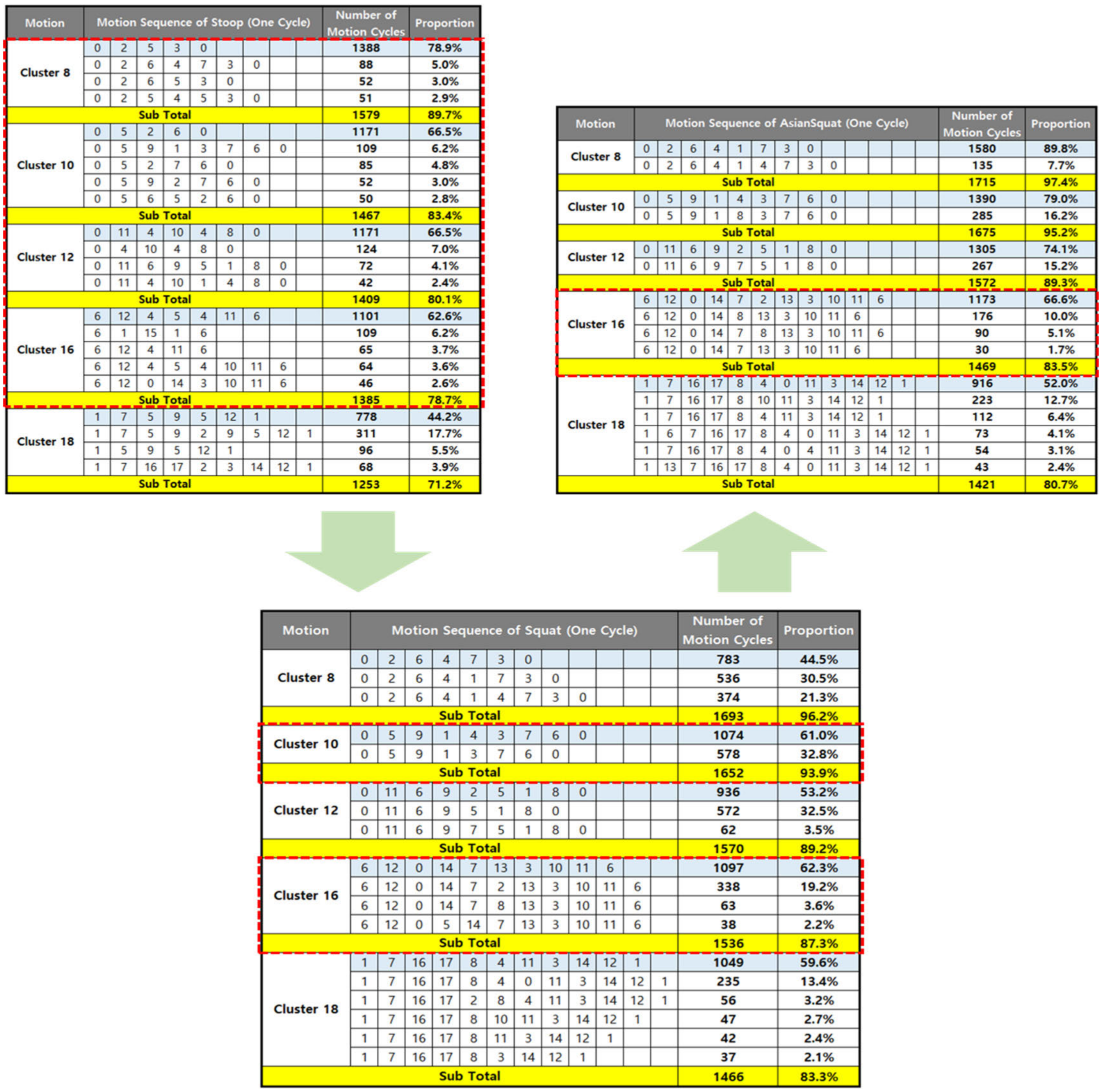

Motion	Motion Sequence of Stoop (One Cycle)									Number of Motion Cycles	Proportion
Cluster 8	0	2	5	3	0					1388	78.9%
	0	2	6	4	7	3	0			88	5.0%
	0	2	6	5	3	0				52	3.0%
	0	2	5	4	5	3	0			51	2.9%
Sub Total										1579	89.7%
Cluster 10	0	5	2	6	0					1171	66.5%
	0	5	9	1	3	7	6	0		109	6.2%
	0	5	2	7	6	0				85	4.8%
	0	5	9	2	7	6	0			52	3.0%
	0	5	6	5	2	6	0			50	2.8%
Sub Total										1467	83.4%
Cluster 12	0	11	4	10	4	8	0			1171	66.5%
	0	4	10	4	8	0				124	7.0%
	0	11	6	9	5	1	8	0		72	4.1%
	0	11	4	10	1	4	8	0		42	2.4%
Sub Total										1409	80.1%
Cluster 16	6	12	4	5	4	11	6			1101	62.6%
	6	1	15	1	6					109	6.2%
	6	12	4	11	6					65	3.7%
	6	12	4	5	4	10	11	6		64	3.6%
	6	12	0	14	3	10	11	6		46	2.6%
Sub Total										1385	78.7%
Cluster 18	1	7	5	9	5	12	1			778	44.2%
	1	7	5	9	2	9	5	12	1	311	17.7%
	1	5	9	5	12	1				96	5.5%
	1	7	16	17	2	3	14	12	1	68	3.9%
Sub Total										1253	71.2%

Motion	Motion Sequence of AsianSquat (One Cycle)													Number of Motion Cycles	Proportion
Cluster 8	0	2	6	4	1	7	3	0						1580	89.8%
	0	2	6	4	1	4	7	3	0					135	7.7%
Sub Total														1715	97.4%
Cluster 10	0	5	9	1	4	3	7	6	0					1390	79.0%
	0	5	9	1	8	3	7	6	0					285	16.2%
Sub Total														1675	95.2%
Cluster 12	0	11	6	9	2	5	1	8	0					1305	74.1%
	0	11	6	9	7	5	1	8	0					267	15.2%
Sub Total														1572	89.3%
Cluster 16	6	12	0	14	7	2	13	3	10	11	6			1173	66.6%
	6	12	0	14	8	13	3	10	11	6				176	10.0%
	6	12	0	14	7	8	13	3	10	11	6			90	5.1%
	6	12	0	14	7	13	3	10	11	6				30	1.7%
Sub Total														1469	83.5%
Cluster 18	1	7	16	17	8	4	0	11	3	14	12	1		916	52.0%
	1	7	16	17	8	10	11	3	14	12	1			223	12.7%
	1	7	16	17	8	4	11	3	14	12	1			112	6.4%
	1	6	7	16	17	8	4	0	11	3	14	12	1	73	4.1%
	1	7	16	17	8	4	0	4	11	3	14	12	1	54	3.1%
	1	13	7	16	17	8	4	0	11	3	14	12	1	43	2.4%
Sub Total														1421	80.7%

Motion	Motion Sequence of Squat (One Cycle)												Number of Motion Cycles	Proportion
Cluster 8	0	2	6	4	7	3	0						783	44.5%
	0	2	6	4	1	7	3	0					536	30.5%
	0	2	6	4	1	4	7	3	0				374	21.3%
Sub Total													1693	96.2%
Cluster 10	0	5	9	1	4	3	7	6	0				1074	61.0%
	0	5	9	1	3	7	6	0					578	32.8%
Sub Total													1652	93.9%
Cluster 12	0	11	6	9	2	5	1	8	0				936	53.2%
	0	11	6	9	5	1	8	0					572	32.5%
	0	11	6	9	7	5	1	8	0				62	3.5%
Sub Total													1570	89.2%
Cluster 16	6	12	0	14	7	13	3	10	11	6			1097	62.3%
	6	12	0	14	7	2	13	3	10	11	6		338	19.2%
	6	12	0	14	7	8	13	3	10	11	6		63	3.6%
	6	12	0	5	14	7	13	3	10	11	6		38	2.2%
Sub Total													1536	87.3%
Cluster 18	1	7	16	17	8	4	11	3	14	12	1		1049	59.6%
	1	7	16	17	8	4	0	11	3	14	12	1	235	13.4%
	1	7	16	17	2	8	4	11	3	14	12	1	56	3.2%
	1	7	16	17	8	10	11	3	14	12	1		47	2.7%
	1	7	16	17	8	11	3	14	12	1			42	2.4%
	1	7	16	17	8	3	14	12	1				37	2.1%
Sub Total													1466	83.3%

FIGURE 3. Rocess for selecting the optimal number of clusters. First, for stoop sequence, we excluded Cluster 18 which had less than 1000 motion cycles in the representative motion sequence (ex: representative motion sequence for Cluster 8 is [0], [2], [5], [3], [0]). Next, for squat sequence, two clusters with a high motion sequence classification rate (above 60%) were selected. Finally, for asiansquat, Cluster 16 which has the largest number of motion elements constituting the motion sequence, was determined as the optimal cluster.

The prediction time for motion intention using minimal initial data is limited. However, if the current motion element can be identified with minimal initial data for each element and the next motion element can be predicted based on sequence information, the limitation on prediction time can be mitigated. Additionally, during the control process of the

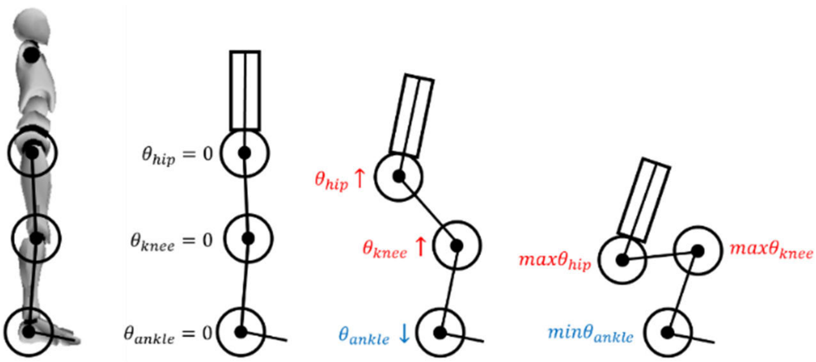

FIGURE 4. Joint angle change according to posture change.

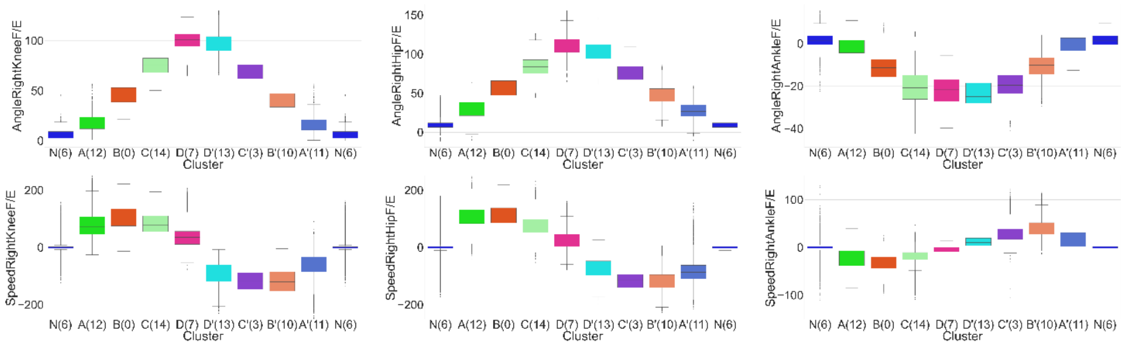

FIGURE 5. Angle and angular velocity values for the squat.

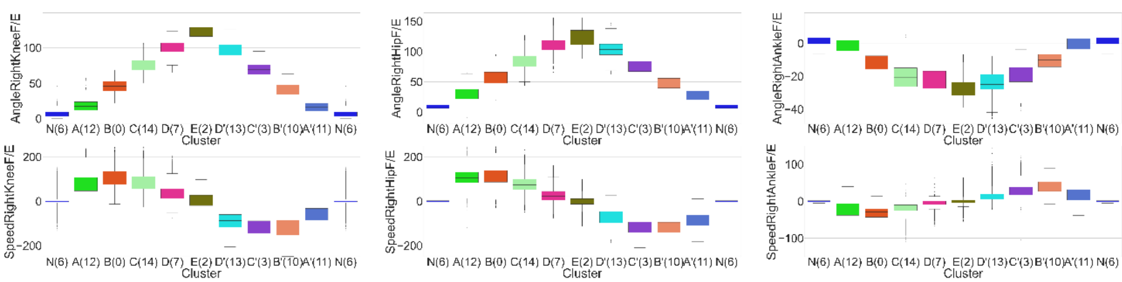

FIGURE 6. Angle and angular vlocity values for the AsianSquat.

Motion	K-Means Clustering													Multi-Layer-Perceptron														
	Motion Sequence (One Cycle)											Number of Motion Cycles	Proportion	Motion Sequence (One Cycle)													Number of Motion Cycles	Proportion
Squat	N	A	B	C	D	D'	C'	B'	A'	N		1097	62.3%	N	A	B	C	D	D'	C'	B'	A'	N				199	66.3%
	N	A	B	C	D	E	D'	C'	B'	A'	N	338	19.2%	N	A	B	C	D	E	D'	C'	B'	A'	N			51	17.0%
	N	A	B	C	D	F	D'	C'	B'	A'	N	63	3.6%	N	A	B	C	D	D'	C'	B'	A'	A	N			12	4.0%
	N	A	B	H	C	D	D'	C'	B'	A'	N	38	2.2%	N	A	B	C	D	E	D	D'	C'	B'	A'	N		8	2.7%
Sub Total												1536	87.3%	Sub Total													270	90.0%
AsianSquat	N	A	B	C	D	E	D'	C'	B'	A'	N	1173	66.6%	N	A	B	C	D	E	D'	C'	B'	A'	N			241	80.3%
	N	A	B	C	F	D'	C'	B'	A'	N		176	10.0%	N	A	B	C	D	E	D	E	D'	C'	B'	A'	N	11	3.7%
	N	A	B	C	D	F	D'	C'	B'	A'	N	90	5.1%	N	A	B	C	D	E	D'	C'	B'	A'	A	N		5	1.7%
	N	A	B	C	D	D'	C'	B'	A'	N		30	1.7%															
Sub Total												1469	83.5%	Sub Total													257	85.7%

FIGURE 7. Table for the identified elements of the human lower extremity motion sequence from unsupervised learning and supervised learning.

exoskeleton robot's actuators, time delays occur due to signal measurement, calculation, and actuator response [6]. Therefore, it is necessary to assess whether each motion element has sufficient execution time.

To begin, the average and standard deviation of the execution time for each motion element were determined. As shown in Table 7, the execution time of the motion element corresponding to the representative sequence was confirmed,

TABLE 7. Average execution time for each motion element.

Movement	Cluster	Execution time (ms)
Squat	N	0.66 ± 1.248
	A	0.244 ± 0.05
	A'	0.236 ± 0.078
	B	0.228 ± 0.051
	B'	0.223 ± 0.042
	C	0.329 ± 0.115
	C'	0.249 ± 0.063
	D	0.548 ± 0.308
	D'	0.256 ± 0.069
AsianSquat	N	0.366 ± 0.82
	A	0.214 ± 0.049
	A'	0.214 ± 0.471
	B	0.228 ± 0.051
	B'	0.208 ± 0.037
	C	0.253 ± 0.064
	C'	0.21 ± 0.042
	D	0.326 ± 0.164
	D'	0.267 ± 0.07
	E	0.813 ± 0.365

TABLE 8. Performance evaluation results of the MLP model.

Metrics	Values
Loss	0.0037
Accuracy	96.17%
Val_Loss	0.0027
Val_Accuracy	97.13%

and it was found that all motion elements lasted more than 200ms.

D. PREDICTION OF THE MOTION ELEMENTS USING THE MLP MODEL

The results obtained from the unsupervised learning model were utilized by the MLP model, and the optimal parameter information is presented in Table 8. These results were then used to predict the data labels for five subjects who were not included in the unsupervised learning process. A total of 600 Squat and AsianSquat movements were analyzed (300 for each movement), and the application of the MLP model indicated that there were 270 meaningful combinations of motion elements for the Squat and 257 for the AsianSquat. This implies that the representative motion sequence for each movement aligned with the results obtained from unsupervised learning, resulting in high classification accuracy. Furthermore, a comparison between the outcomes of unsupervised learning and supervised learning can be observed in Figure 7.

V. DISCUSSION

In this study, the goal was to implement proactive control of an exoskeleton robot by deriving motion elements for lower extremity motions. These motions were expressed as sequences to predict natural robot control and motion intentions without causing inconvenience to humans. A previous study [10] has demonstrated the effectiveness of segmenting motion into six types based on selected features from real-time bio-signal data, enabling a better understanding of the motion sequence as a whole. However, no additional studies using Naghdy and Fazel [10] research method were found. This is likely due to the recent advancements in bio-signal measuring sensors and machine learning technology, which allow for deriving results from sensor data using artificial intelligence algorithms. Hence, controlling the exoskeleton robot by identifying the motion sequence through the motion segmentation technique aligns with the research method and can be effective. The significance of this study lies in demonstrating that proactive control of an exoskeleton robot can be achieved by dividing movements into elements, processing a larger amount of data compared to previous studies, and expressing lower extremity motion as a sequence. The results of this study can guide future research on implementing proactive control of an exoskeleton robot.

Several previous studies have highlighted the importance of nullifying control delay time for proactive robot control [6], [20], [23]. Motion mismatch issues may persist when implementing proactive control without compensating for control delay time. Ding et al. [6] suggested that to control an exoskeleton, it is necessary to predict motion at least 124ms ahead considering the control delay time when utilizing past 200ms of data. To compare our results with Ding et al., Table 7 confirms that the execution time for all motion elements constituting the representative sequence exceeds 200ms. This indicates the possibility of predicting an operation after 124ms by using 200ms of initial data for each element operation. Additionally, Beil et al. [20] conducted a study on control delay time by varying the time of using past data to control the exoskeleton robot. Considering the data duration and model accuracy, using 300ms of past data was deemed optimal, suggesting a control delay time of 368.97ms. This implies that motion prediction should be made after approximately three times the control delay time suggested by Ding et al. [6]. However, Beil et al.'s study employed a total of 39 features, whereas our study utilized 18 features, potentially saving data calculation time. Given the significant advancements in sensor performance, the temporal aspect can be supplemented using the results of this study. Therefore, proactive control can be implemented by predicting the motion intention of the exoskeleton robot.

In this study, IMU sensor was used to derive motion elements for lower extremity motions. By applying feature reduction, only 18 features out of 42 were employed to segment the lower extremity motion into 11 motion elements. The angle and speed (angular velocity) values of each motion element were analyzed, revealing certain elements that were paired and were symmetrical. Thus, the possibility of proactive control was confirmed by defining new symbols for motion elements and expressing the sequence of lower extremity motion. However, the results indicate that the motion element distinguishing Squat and

TABLE 9. Divided range of the knee angle of the motion elements.

	N	A-A'	B-B'	C-C'	D-D'	E
Case 1	0~8	8~25	25~55	55~85	85~110	110~155
Case 2	0~10	10~30	30~60	60~90	90~110	110~155
Case 3	0~10	10~30	30~60	60~90	90~120	120~155

(A)

Motion	Multi-Layer-Perceptron: Motion Sequence (One Cycle)	Number of Motion Cycles	Proportion	Multi-Layer-Perceptron (Case 1): Motion Sequence (One Cycle)	Number of Motion Cycles	Proportion
Squat	N A B C D D' C' B' A' N	199	66.3%	N A B C D D' C' B' A' N	190	63.3%
	N A B C D E D' C' B' A' N	51	17.0%	N A B C D E D' C' B' A' N	51	17.0%
	N A B C D D' C' B' A' A N	12	4.0%			
	N A B C D E D D' C' B' A' N	8	2.7%			
Sub Total		270	90.0%	Sub Total	241	80.3%
AsianSquat	N A B C D E D' C' B' A' N	241	80.3%	N A B C D E D' C' B' A' N	201	67.0%
	N A B C D E D E D' C' B' A' N	11	3.7%	N A B C D E D E D' C' B' A' N	13	4.3%
	N A B C D E D' C' B' A' A N	5	1.7%			0.0%
Sub Total		257	85.7%	Sub Total	214	71.3%

(B)

Motion	Multi-Layer-Perceptron: Motion Sequence (One Cycle)	Number of Motion Cycles	Proportion	Multi-Layer-Perceptron (Case 2): Motion Sequence (One Cycle)	Number of Motion Cycles	Proportion
Squat	N A B C D D' C' B' A' N	199	66.3%	N A B C D D' C' B' A' N	200	66.7%
	N A B C D E D' C' B' A' N	51	17.0%	N A B C D E D' C' B' A' N	68	22.7%
	N A B C D D' C' B' A' A N	12	4.0%			
	N A B C D E D D' C' B' A' N	8	2.7%			
Sub Total		270	90.0%	Sub Total	268	89.3%
AsianSquat	N A B C D E D' C' B' A' N	241	80.3%	N A B C D E D' C' B' A' N	230	76.7%
	N A B C D E D E D' C' B' A' N	11	3.7%	N A B C D E D E D' C' B' A' N	17	5.7%
	N A B C D E D' C' B' A' A N	5	1.7%	N A B C D D' C' B' A' N	13	4.3%
Sub Total		257	85.7%	Sub Total	260	86.7%

(C)

Motion	Multi-Layer-Perceptron: Motion Sequence (One Cycle)	Number of Motion Cycles	Proportion	Multi-Layer-Perceptron (Case 3): Motion Sequence (One Cycle)	Number of Motion Cycles	Proportion
Squat	N A B C D D' C' B' A' N	199	66.3%	N A B C D D' C' B' A' N	221	73.7%
	N A B C D E D' C' B' A' N	51	17.0%	N A B C D E D' C' B' A' N	20	6.7%
	N A B C D D' C' B' A' A N	12	4.0%			
	N A B C D E D D' C' B' A' N	8	2.7%			
Sub Total		270	90.0%	Sub Total	241	80.3%
AsianSquat	N A B C D E D' C' B' A' N	241	80.3%	N A B C D E D' C' B' A' N	158	52.7%
	N A B C D E D E D' C' B' A' N	11	3.7%	N A B C D E F D' C' B' A' N	40	13.3%
	N A B C D E D' C' B' A' A N	5	1.7%	N A B C D D' C' B' A' N	31	10.3%
Sub Total		257	85.7%	Sub Total	229	76.3%

FIGURE 8. Supervised learning results with respect to three cases of the divided range of knee angle of the motion elements.

AsianSquat is "E". It remains challenging to determine from the prediction results whether a human will perform a Squat or an AsianSquat, even with information about the motion sequence. Furthermore, predicting and controlling different human motion intentions innately is complex since the results are based on data from predetermined experimental motions. To address these limitations, future studies could incorporate EMG or insole sensors, as previous research has suggested [6], [20], [23], [33], to predict motion intention in addition to the IMU sensor.

Another aspect that should be considered is setting the range of motion (ROM) for each motion element's knee to understand motion intentions and facilitate prediction. Therefore, as shown in Table 9, the ROM for each motion element was divided into three cases. Case 1 involved setting the range based on the 1st and 3rd quartiles, Case 2 utilized average values, and Case 3 used average values but with a larger range for 'D'. Through unsupervised learning, only the ROM data for each case was altered and trained using the MLP model, yielding the results shown in Figure 8. When the ROM was changed as in Case 2, the prediction closely matched the existing MLP prediction result. This suggests that even if the knee angle for each motion element is adjusted to avoid overlap, a similar model performance can be achieved. These findings indicate that the exoskeleton robot can be controlled based on the worker's knee angle.

VI. CONCLUSION

This study identified a problem in the industrial field, which is the mismatch between the worker's motion intention and the control of the exoskeleton. To address this issue, proactive control that considers control delay time must be implemented. Understanding human motion intention is crucial for proactive control, and thus, a study applying the motion segmentation technique to IMU sensor data was conducted to identify the motion elements of lower extremity motion. Using the IMU data, the lower extremity motion was segmented into 11 meaningful motion elements using the k-means clustering algorithm. These 11 motion elements allowed the expression of Squat and AsianSquat movements as a sequence. Additionally, the potential for developing a motion intention and sequence prediction model was verified through training an MLP model and predicting the motion sequence of new data. Notably, the duration of each motion element in the sequence exceeded 200ms, establishing the feasibility of proactive control using the motion segmentation technique for the exoskeleton.

To overcome the limitations of the proposed approach, further explorations based on the findings of this study are necessary in the next stage. Firstly, the motion intention should be identified based on the initial data of each motion element. This is because it is necessary to check how far ahead the motion intention and sequence prediction model can predict the motion intention using only a single IMU sensor. Afterwards, the goal is to compensate for the control delay time of more than 300ms by additionally using an EMG sensor data and to secure the synchrony of movement intention and control. As a result, we aim to develop a proactive control algorithm for a multimodal sensor-based exoskeleton robot. On the other hand, we are currently researching healthy men in their 20s targeting lifting movements among lower extremity movements, but in the future, we will diversify movements such as walking, lunging, and going up and down stairs. We also plan to conduct additional experiments to examine the subjects' characteristics (age, height, weight, gender, etc.). It is expected that proactive control can be sufficiently implemented if the corresponding actions are expressed as a sequence using the movement segmentation technique.

In this way, after developing a proactive control algorithm for an exoskeleton robot that can assist various lower limb movements, the verification and evaluation process of the algorithm must be performed through the actual exoskeleton robot or simulation. One of the important issues in exoskeleton research is to accurately identify the operator's movement intention in real-time and implement effective control [31]. Accordingly, it is necessary to verify the algorithm's performance by compensating the control delay time and whether control starts simultaneously with the human motion intention. Additionally, since safety is an important factor when evaluating the performance of an exoskeleton, control instability caused by the algorithm must be minimized [32]. To address these issues, Akbari et al. [11] proposed a method to evaluate the uncertainty of a deep learning algorithm in real time and use this uncertainty measurement in the robot's control loop to update the system whenever an unsafe situation for the user occurs. In [33], an adaptive intention-based variable impedance controller was proposed to estimate human motion intentions online based on physical interactions, stochastic distributions, and random disturbances by Huo, Y. et al. As such, since exoskeleton robots are worn by humans, it will be essential to solve the problem of false detections caused by algorithms. In the future, after developing a multi-modal sensor-based motion intention prediction algorithm, we will secure safety by establishing a response strategy in case of false detection of the algorithm, as in previous studies.

REFERENCES

[1] A. M. Dollar and H. Herr, "Lower extremity exoskeletons and active orthoses: Challenges and state-of-the-art," *IEEE Trans. Robot.*, vol. 24, no. 1, pp. 144–158, Feb. 2008.

[2] K. Anam and A. A. Al-Jumaily, "Active exoskeleton control systems: State of the art," *Proc. Eng.*, vol. 41, pp. 988–994, Jan. 2012.

[3] E. Trigili, L. Grazi, S. Crea, A. Accogli, J. Carpaneto, S. Micera, N. Vitiello, and A. Panarese, "Detection of movement onset using EMG signals for upper-limb exoskeletons in reaching tasks," *J. Neuroeng. Rehabil.*, vol. 16, no. 1, pp. 1–16, Dec. 2019.

[4] E. Maxheimer, C. Shanahan, A. Wolf, J. Craig, D. Mountjoy, C. Johnson, and D. Canzonetta, "A human systems integration approach to industrial exoskeleton evaluations for the USAF," 711th Hum. Perform. Wing, Wright-Patterson Air Force Base, OH, USA, Oct. 2019.

[5] C.-H. Kuo, J.-W. Chen, Y. Yang, Y.-H. Lan, S.-W. Lu, C.-F. Wang, Y.-C. Lo, C.-L. Lin, S.-H. Lin, P.-C. Chen, and Y.-Y. Chen, "A differentiable dynamic model for musculoskeletal simulation and exoskeleton control," *Biosensors*, vol. 12, no. 5, p. 312, May 2022.

[6] M. Ding, M. Nagashima, S.-G. Cho, J. Takamatsu, and T. Ogasawara, "Control of walking assist exoskeleton with time-delay based on the prediction of plantar force," *IEEE Access*, vol. 8, pp. 138642–138651, 2020.

[7] G. Pfurtscheller, C. Guger, G. Müller, G. Krausz, and C. Neuper, "Brain oscillations control hand orthosis in a tetraplegic," *Neurosci. Lett.*, vol. 292, no. 3, pp. 211–214, Oct. 2000.

[8] A. Ubeda, E. Iañez, and J. M. Azorin, "Wireless and portable EOG-based interface for assisting disabled people," *IEEE/ASME Trans. Mechatronics*, vol. 16, no. 5, pp. 870–873, Oct. 2011.

[9] R. M. Singh, S. Chatterji, and A. Kumar, "Trends and challenges in EMG based control scheme of exoskeleton robots—A review," *Int. J. Sci. Eng. Res.*, vol. 3, no. 8, pp. 933–940, Aug. 2012.

[10] F. Naghdy, "Fuzzy clustering of human motor motion," *Appl. Soft Comput.*, vol. 11, no. 1, pp. 927–935, Jan. 2011.

[11] M. Akbari, J. K. Mehr, L. Ma, and M. Tavakoli, "Uncertainty-aware safe adaptable motion planning of lower-limb exoskeletons using random forest regression," *Mechatronics*, vol. 95, Nov. 2023, Art. no. 103060.

[12] B. Krüger, A. Vögele, T. Willig, A. Yao, R. Klein, and A. Weber, "Efficient unsupervised temporal segmentation of motion data," *IEEE Trans. Multimedia*, vol. 19, no. 4, pp. 797–812, Apr. 2017.

[13] X. Yu, W. Liu, and W. Xing, "Behavioral segmentation for human motion capture data based on graph cut method," *J. Vis. Lang. Comput.*, vol. 43, pp. 50–59, Dec. 2017.

[14] G. Xia, H. Sun, L. Feng, G. Zhang, and Y. Liu, "Human motion segmentation via robust kernel sparse subspace clustering," *IEEE Trans. Image Process.*, vol. 27, no. 1, pp. 135–150, Jan. 2018.

[15] S. Li, K. Li, and Y. Fu, "Temporal subspace clustering for human motion segmentation," in *Proc. IEEE Int. Conf. Comput. Vis. (ICCV)*, Dec. 2015, pp. 4453–4461.

[16] F. Zhou, F. De la Torre, and J. K. Hodgins, "Hierarchical aligned cluster analysis for temporal clustering of human motion," *IEEE Trans. Pattern Anal. Mach. Intell.*, vol. 35, no. 3, pp. 582–596, Mar. 2013.

[17] C.-S. Lee and A. Elgammal, "Human motion synthesis by motion manifold learning and motion primitive segmentation," in *Proc. 4th Int. Conf. Articulated Motion Deformable Objects*, vol. 4, Mallorca, Spain, Jul. 2006, pp. 464–473.

[18] G. Clark and H. B. Amor, "Learning ergonomic control in human–robot symbiotic walking," *IEEE Trans. Robot.*, vol. 39, no. 1, pp. 327–342, Feb. 2023.

[19] J. Ryu, T. McFarland, C. T. Haas, and E. Abdel-Rahman, "Automatic clustering of proper working postures for phases of movement," *Autom. Construct.*, vol. 138, Jun. 2022, Art. no. 104223.

[20] J. Beil, I. Ehrenberger, C. Scherer, C. Mandery, and T. Asfour, "Human motion classification based on multi-modal sensor data for lower limb exoskeletons," in *Proc. IEEE/RSJ Int. Conf. Intell. Robots Syst. (IROS)*, Oct. 2018, pp. 5431–5436.

[21] M. Zhang and A. A. Sawchuk, "Motion primitive-based human activity recognition using a bag-of-features approach," in *Proc. 2nd ACM SIGHIT Int. Health Informat. Symp.*, Jan. 2012, pp. 631–640.

[22] P. Santikan, W. Tangwongcharoen, and W. Kimpan, "Define stance and swing pattern of gait cycle using motion sensor and K-mean clustering," in *Proc. 19th Int. Conf. Electr. Eng./Electron., Comput., Telecommun. Inf. Technol. (ECTI-CON)*, May 2022, pp. 1–4.

[23] S. Tortora, S. Michieletto, F. Stival, and E. Menegatti, "Fast human motion prediction for human–robot collaboration with wearable interface," in *Proc. IEEE Int. Conf. Cybern. Intell. Syst. (CIS) IEEE Conf. Robot., Autom. Mechatronics (RAM)*, Nov. 2019, pp. 457–462.

[24] R. Stolyarov, G. Burnett, and H. Herr, "Translational motion tracking of leg joints for enhanced prediction of walking tasks," *IEEE Trans. Biomed. Eng.*, vol. 65, no. 4, pp. 763–769, Apr. 2018.

[25] B. Fang, Q. Zhou, F. Sun, J. Shan, M. Wang, C. Xiang, and Q. Zhang, "Gait neural network for human-exoskeleton interaction," *Frontiers Neurorobot.*, vol. 14, p. 58, Oct. 2020.

[26] N. A. Mat Isa, S. A. Salamah, and U. K. Ngah, "Adaptive fuzzy moving K-means clustering algorithm for image segmentation," *IEEE Trans. Consum. Electron.*, vol. 55, no. 4, pp. 2145–2153, Nov. 2009.

[27] T. W. Pribadi and T. Shinoda, "Hand motion recognition of shipyard welder using 9-DOF inertial measurement unit and multi layer perceptron approach," *IOP Conf. Ser., Earth Environ. Sci.*, vol. 557, no. 1, Aug. 2020, Art. no. 012009.

[28] D.-X. Liu, X. Wu, W. Du, C. Wang, and T. Xu, "Gait phase recognition for lower-limb exoskeleton with only joint angular sensors," *Sensors*, vol. 16, no. 10, p. 1579, Sep. 2016.

[29] D. S. Pamungkas, W. Caesarendra, H. Soebakti, R. Analia, and S. Susanto, "Overview: Types of lower limb exoskeletons," *Electronics*, vol. 8, no. 11, p. 1283, Nov. 2019.

[30] J. Hwang, H. Shin, and M.-C. Jung, "Joint motion pattern classification by cluster analysis of kinematic, demographic, and subjective variables," *Appl. Ergonom.*, vol. 44, no. 4, pp. 636–642, Jul. 2013.

[31] Z. Chen, Q. Guo, T. Li, Y. Yan, and D. Jiang, "Gait prediction and variable admittance control for lower limb exoskeleton with measurement delay and extended-state-observer," *IEEE Trans. Neural Netw. Learn. Syst.*, vol. 34, no. 11, pp. 8693–8706, Nov. 2023.

[32] Z. Chen, Q. Guo, T. Li, and Y. Yan, "Output constrained control of lower limb exoskeleton based on knee motion probabilistic model with finite-time extended state observer," *IEEE/ASME Trans. Mechatronics*, vol. 28, no. 4, pp. 2305–2316, Aug. 2023.

[33] Y. Huo, X. Li, X. Zhang, X. Li, and D. Sun, "Adaptive intention-driven variable impedance control for wearable robots with compliant actuators," *IEEE Trans. Control Syst. Technol.*, vol. 31, no. 3, pp. 1308–1323, May 2023.

JONG-HA WOO received the B.S. degree in industrial engineering from the Kumoh National Institute of Technology (KIT), Gumi, South Korea, in 2017, where he is currently pursuing the master's degree in industrial engineering. His research interests include human–robot interaction, ergonomics, interaction design, and data science.

K. KRISHNA SAHITHI received the B.Tech. degree in electronics and communication engineering from SASTRA Deemed University, India, in 2018. She is currently pursuing the master's degree in industrial engineering with the Kumoh National Institute of Technology (KIT), Gumi, South Korea. Her research interests include emotional engineering, human–robot interaction, usability engineering, eXtended reality, and quality of experience research.

SEONG-TAEK KIM is currently pursuing the B.S. degree in industrial engineering with the Kumoh National Institute of Technology (KIT), Gumi, South Korea. His research interests include ergonomics, human–computer interaction, and human–robot interaction.

GEUN-RYEONG CHOI is currently pursuing the B.S. degree in industrial engineering with the Kumoh National Institute of Technology (KIT), Gumi, South Korea. Her research interests include human–robot interaction, eXtended reality, and in-vehicle infotainment systems.

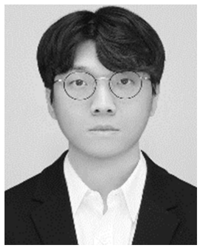

BEOM-SU KIM received the B.S. degree in industrial engineering from the Kumoh National Institute of Technology (KIT), Gumi, South Korea, in 2022, where he is currently pursuing the master's degree in industrial engineering. His research interests include human–robot interaction, ergonomics, interaction design, and data science.

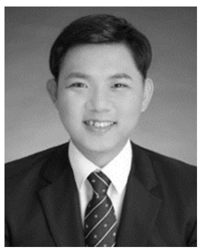

JONG-GYU SHIN received the B.S., M.S., and Ph.D. degrees in industrial engineering from the Kumoh National Institute of Technology (KIT), Gumi, South Korea, in 2015, 2017, and 2021, respectively. He is currently a Postdoctoral Researcher with the Research Institute of Industrial Engineering and Management, KIT. His research interests include ergonomics, emotional engineering, usability engineering, and human–robot interaction.

SANG-HO KIM received the B.S. degree in industrial engineering from Sungkyunkwan University, Seoul, South Korea, in 1989, and the M.S. and Ph.D. degrees in industrial engineering from the Pohang University of Science and Technology (POSTECH), Pohang, South Korea, in 1991 and 1995, respectively. He is currently a Professor with the Department of Industrial Engineering, Kumoh National Institute of Technology (KIT), Gumi, South Korea. His research interests include occupational safety engineering, interaction design, ergonomics, human–robot interaction, emotional engineering, and usability engineering.